University of Nevada, Reno

Actin-Myosin Kinetics and the Effect of Myosin Binding on Cooperative Thin Filament Activation

By,

Samuel P. Dugan

Dr. Josh Baker and Dr. Milad Webb, Thesis Advisors

May 2013

Abstract- Activation of the acto-myosin complex is controlled by the regulatory proteins tropomyosin (Tm) and troponin (Tn) which is made up of the C, I and T subunits. TnC undergoes a conformational change upon calcium binding triggering the release of actin by TnI thereby allowing the TmTn complex to move away from myosin binding sites. This process is known as regulation. Regulation allows for what is known as cooperativity, or the ability of a single initial event to make a subsequent event more or less likely. As this relates to muscle mechanics cooperativity is defined in two ways, these being calcium sensitive and myosin dependent respectively. With regard to myosin dependency cooperativity is a measure of the ability of one myosin head binding the thin filament to increase the chances of another myosin head binding to the thin filament and is therefore related to the number of myosin heads bound to the thin filament (N_b). Cooperativity is related to calcium sensitivity in that the regulatory complex must move away from the actin binding sites for a myosin head to bind. In addition to myosin dependent this becomes calcium dependent with the binding of calcium to the TnC subunit of Tn. *In vitro* motility assays were used to study the cooperative nature of thin filament activation measuring the velocity of the actin+TmTn complex. Velocities of the thin filament were measured while varying myosin density, pCa, and at constant myosin density varying pCa with results showing that with increasing myosin concentration there is a decrease in cooperativity based on the Hill function cooperative coefficient. In addition this shows an increase in pCa_{50}, or the concentration of calcium at which we attain half maximal velocity of the thin filament. With a decrease in myosin density there is an increase in cooperativity and a subsequent decrease in pCa_{50} . This pCa_{50} value is known to be affected by the duty ratio, whereas cooperativity is again a function of N_b. In addition the effects of phosphate on the binding pathway of unregulated myosin were studied again using an *in vitro* motility assay

varying the concentration of myosin density and the presence of phosphate. Experiments were

performed using rabbit striated muscle. Additional studies of the binding pathways of actin-

myosin interactions were done using *N,N'p*-phenylenedimaleimide (pPDM) which is a structural

analogue of myosin subfragment-1 thought to force actin-myosin interaction towards a weakly

bound state (14).

Table of Contents

List of Figures

List of Illustrations

Actin-Myosin Kinetics and the Effect of Myosin Binding on Cooperative Thin Filament Activation

Introduction- The thin filament of striated muscle is activated by both calcium binding to a regulatory protein complex, and myosin heads binding to the thin filament which leads to the contraction of muscle as the thin and thick filaments slide past each other. The regulatory proteins that control this process are known as troponin (Tn) and tropomyosin (Tm). Tn is composed of three subunits, C, I, and T and upon calcium binding of the C subunit the TnI subunit changes conformation to an open E-F hands conformation of the TnC subunit. This allows for the movement of the TmTn complex off of the myosin binding sites on the thin filament. This brings about a partially blocked calcium induced state that allows for activation of the thin filament upon myosin binding. Such binding further displaces Tm from the binding sites along the thin filament. We have thus established the premise for both calcium and myosin dependent activation of the thin filament and through regulation, have established a mechanism through which cooperativity could affect activation of the thin filament. For the purposes of this paper we will define cooperativity as the ability of a single event to make a subsequent event more or less likely.

Common models, such as those proposed by Geeves, discuss activation through a structural perspective in which there exist distinct states of activation that are in effect, separated from each other without regard for the physiological transition between such states. In contrast we will explore a more simple model of thin filament regulation (SCoR) that includes the assumption that kinetics and structural dynamics work hand in hand when transitioning from a deactivated to activated state. We will explore this transition as an integrated process of kinetics and structure described by the rate constant k_{att}. This being a chemical representation of thin filament activation, it is dependent on the assumptions that the calcium/myosin dependent

variations in structure are accounted for in the dependence of k_{att} upon calcium and myosin. This is based in part on the assumption that calcium dependence of k_{att} follows a Hill function. A further assumption stipulates that myosin activation of k_{att} is maximally activated when N_b is greater than or equal to 1. However, because of the cooperative nature of myosin activation we develop a simple concerted model of regulation (SCoR) in which k_{att} increases with an increase in N_b.

We show that SCoR accurately predicts a novel relationship between k_{att}, k_{det}, N and pCa_{50}. This is based in SCoR's ability to predict a linear variation in pCa_{50} with N(r) where N is the number of available myosin heads binding a thin filament and r is the myosin duty ratio at maximal activation $\left(\frac{\tau_{on}}{\tau_{on}+\tau_{off}}\right)$. This is tested through the use of an *in vitro* motility assay in which the speed, V, of the thin filament as it moves over a bed of myosin is measured and used as an indicator of the level of activation of the thin filament. Various inhibitors of k_{att} and k_{det} are used and the concentration of calcium is varied to determine their respective affects on activation. Results show that a change in any of these parameters results in a corresponding change in pCa_{50} that is proportional to the change in N(r). In addition any change that returns *N(r)* to its original value will restore pCa_{50} to its corresponding value.

We will also discuss the effect of phosphate on the transition from unbound to strongly bound states. There has been detected in muscle fibers a weakly bound state (15). Thus there would seem to be two possible pathways to achieve a myosin-actin strongly bound state. These being, a transition from dissociated to strongly bound through an intermediate weakly bound state, or a single transition from dissociated to strongly bound (figure 15). Weakly bound states could become saturated with only a few of these states transitioning to strongly bound productive

states. However there is some debate about whether or not this weakly bound state actually lies on the path from unbound to strongly bound actomyosin interactions (15). With addition of phosphate, sliding velocity/ATPase cycle actually slows when compared to a control curve varying only myosin density. This suggests two things, one being that there is a saturation of productive myosin heads at high concentrations of myosin, and two, that multiple weakly bound transition states can become saturated with addition of phosphate and high myosin concentrations thus slowing velocity. In addition this might provide insight into whether or not the weakly bound state is actually on the pathway to strong binding or merely a momentary association between actin and myosin. Evidence for this can be found through an *in vitro* motility assay that shows a departure from maximally activated thin filaments with addition of phosphate to varying myosin density.

In addition a brief study of the effects of *N,N'p*-phenylenedimaleimide (pPDM) modified myosin S-1, which is thought to push actin and myosin towards a weakly bound state (*14*), was done to discern effects of ionic drag on activation.

The goal of this thesis is to provide insight, including novel predictions, into the role that calcium sesnsitivity, myosin dependent activation and cooperativity, and attachment/detachment kinetics have in the role of cardiac and skeletal muscle contraction. In short our research shows that, through modulation of duty ratio and tuning of calcium sensitivity cardiac and skeletal muscle contraction could potentially be restored to normal conditions in disease causing states. In addition we provide preliminary evidence that a structural weak binding transition state may become saturated with addition of phosphate thus slowing sliding velocity at higher (load inducing) myosin concentrations. In addition there is preliminary evidence that a weak binding transition state may not be necessary to achieve strong binding. A greater understanding of the

roles of calcium/myosin activation and cooperativity can be applied to further studies of thin filament regulation. Direct modulation of these effects by changing duty ratio or myosin concentration could lead to effective therapeutic treatment of specific cardiomyopathies or loss of function mutations in cardiac and skeletal muscle.

Methods-

Buffers

The myosin buffer was made using 300mM KCL, 25mM imidazole, 1mM EGTA, 4 mM $MgCl_2$, and 10 mM DTT. Actin buffer was made using 50 mM KCl, 50 mM imidazole, 2 mM EGTA, 8 mM $MgCl_2$, and 10 mM DTT. For in vitro motility experiments the motility buffer was used at 1 mM ATP. Motility buffer contained 25 nM TmTn, 50 mM KCl, 50 mM imidazole, 2 mM EGTA, 8 mM $MgCl_2$, 10 mM DTT, 0.5% methylcellulose. Stock solutions of sucrose were made by dissolving >99.5% pure sucrose, (Sigma-Aldrich, St. Louis, MO) to a concentration of 80% in distilled water. Amrinone (Sigma-Aldrich, St. Louis, MO) was prepared in 0.5 M lactic acid at a concentration of 214 mM, as previously described (1). Buffers were used at a pH of 7.4 achieved through the use of NaOH. Buffers had oxygen scavenger added to them immediately before imaging (~6 mg/ml glucose, 0.03 mg/ml glucose oxidase, 0.05 mg/ml catalase) to minimize the effect it would have on the pH of the motility buffers.

Proteins

Skeletal muscle myosin was prepared from a rabbit psoas muscle as previously described and stored in glycerol at $-20°C$ (*4,5*). Actin was then purified from rabbit psoas and stored on

ice at 4℃ (*6*). In vitro motility assays used 1 µM actin that was incubated with 1 µM

tetramethyl-rhodamine isothiocyanate (TRITC) phalloidin overnight at 4℃. Troponin and

tropomyosin (TmTn) were purified from rabbit skeletal muscle as previously described (*2*, *3*). 1

µM actin was incubated with 100 nM TmTn for 10-15 minutes prior to use.

In vitro motility assays

Velocities of fluorescently labeled actin thin filaments were measured as they slid over a

bed of myosin heads in an in vitro motility assay at 30℃. Flow cells were made by attaching a

nitrocellulose coated coverslip to a microscope slide with double sided ¼ inch, 5 mils thick

tape (3M, St. Paul, MN). Myosin, at a concentration of 100 µg/ml was applied to the flow cell

and was followed by the application of 5 mg/ml BSA and 10 nM TRITC-actin. Each of these

reagents was incubated for a period of 2 minutes before addition of the next. Finally flow cells

were washed with an actin buffer prior to addition of the motility buffer. Motility assays were

performed using a Nikon TE2000 epifluorescence microscope with fluorescence images digitally

acquired with a Roper Cascade 512B camera (Princeton Instruments, Trenton, NJ). Each flow

cell provided three separate 30 second image recordings from three different fields containing

roughly 20-40 actin filaments. Data from these three separate fields constituted a one (n=1)

experiment.

Image Tracking

For each sequence of images objects were segmented from the background using binary

threshold and their positions calculated using SimplePCI software for Image Acquisition and

Analysis (Hamamatsu Corporation, Sewickley, PA) IPA-MTA (Motion Tracking and Analysis)

centroid algorithm. Trajectories of intersecting filaments were excluded and a minimum distance of 5 μm was required to filter smoothly moving filaments.

SCoR Predictions

A simple concerted model of regulation or SCoR was used to predict relationships between changes in duty ratio and a subsequent shift in pCa. The simulation was based on a two state model and transition probabilities for actin-myosin attachment and detachment were determined from parameters for attachment $N{\cdot}k_{att}'$ (Eq. 1) and detachment, k_{det}, kinetic rates, where N is the number of available myosin heads for binding an actin thin filament. Fractional activation of the thin filament was determined at each step and averaged over the simulation to get an average velocity for that simulation as described in equations 1-3. Each simulated velocity was obtained from an average of ten 50 second simulations. Simulated calcium dependence of velocities was analyzed using a Levenberg=Marquardt minimization algorithm for the Hill function given as $V = V_{min} + \left(\frac{V_{max}-V_{min}}{1+10^{(Log(pCa_0-pCa))n_H}}\right)$. The rate of thin filament-myosin binding (k_{att}') is defined as a fraction of the maximal rate of attachment (k_{att}) by equation 1:

$$k_{att}' = k_{att}\left[\left((f_c)\frac{[Ca^{2+}]^n}{[Ca^{2+}]^n\ +\ K_{Ca}{}^n} + (f_m)\frac{N_b}{N_b\ +\ K_{ma}}\right)\right] + k_{basal}$$

The calcium dependence of k_{att} is calculated as a Hill function, where n is the cooperativity coefficient and K_{ca} is Tn-calcium affinity. The N_b-dependence of k_{att} is based on a hyperbolic function where K_{ma} is the number of bound myosin heads to the thin filament necessary to achieve half maximal myosin activation of the thin filament. The extent to which calcium- and myosin-dependent activation, f_c and f_m respectively, can be influenced by calcium- or myosin-binding alone is given by the fractional contributions in equation 1. This simulation limits k_{att}' to

a maximum value of k_{att}. This then allows for the fractional activation A_f to be defined as equation 2:

$$A_f = \frac{k_{att'}}{k_{att}} \leq 1$$

Simulated sliding velocities are calculated from equation 3:

$$V = d \cdot k_{det} \cdot A_f$$

The assumption is made that the maximal thin filament sliding velocities V_{max} are the product of the average myosin step size (d) and the rate of thin filament-myosin detachment (k_{det}). A partially activated filament's velocity (V) is calculated as the product of V_{max} and A_f.

Results-

Results show the ability of high density myosin to activate the thin filament at subactivating concentrations of calcium (figure 14). Having established the ability of myosin to activate the thin filament at subactivating concentrations of calcium varying myosin concentrations in *in vitro* motility assays yields differing slope values when fit with a Hill function. Slopes are greatest when the concentration of myosin is the lowest. As concentration of myosin increases slope values decrease while Vmax values increase (figure 1). When these slope values are plotted as Hill coefficients against concentration of myosin or N_b we see a decrease in the coefficient with increased N_b (figure 2). Further analysis of the effect of duty ratio on cooperativity is shown through the effect of amrinone on the duty ratio (figure 3). Changing the amrinone concentration from 2mM to 4mM decreases the slope of the respective pCa curves. This is compared to a control and as seen addition of amrinone decreases the slope of the pCa curve and thus the calculated Hill coefficients decrease as we increase the concentration of amrinone from 0 to 4mM (figure 4). Taken together these two contributors to actomyosin

kinetics, duty ratio and N_b, we can simulate their effects on cooperativity through the use of the SCoR model outlined previously. We thus multiply the concentration of myosin by the duty ratio and as the product of this increases we see a decrease in the cooperative coefficient as predicted by SCoR (figure 5).

Amrinone and Sucrose have both been shown to shift the pCa_{50} value for in vitro motility curves and this is shown in figures 7 and 8 as compared to the control pCa curve (figure 6). The control curve gives a pCa_{50} value of 6.17 with pCa_{50} being the -log concentration of calcium at which we see half maximal velocity of the thin filament. For our purposes this half maximal velocity corresponds to half maximal activation of the thin filament. A sucrose curve showing compilated values from three different curves shows a rightward shift in the pCa_{50} that is equal to 5.57 (figure 7). This is a higher concentration of calcium at half maximal activation than is seen in the control curve. It was important to show that not only are velocities decreasing as the concentration of calcium is changed but also that the percent of moving filaments decreased as well (figure 8). Amrinone shifts the pCa_{50} value to the left of the control with a value of 6.42 (figure 9). This is a lower calcium concentration to achieve half maximal velocity than we see in the control curve pCa_{50} 6.17 (figure 6). This shows a loss of calcium sensitivity. When combining the use of sucrose (attachment kinetics) and amrinone (detachment kinetics) (figure 10) SCoR predicts a recovery of calcium sensitivity measured in pCa_{50} value. With addition of 4mM amrinone and 120mM sucrose we see a recovery of pCa_{50} value to 5.64 and 5.66. This supports our model predictions of altered attachment-detachment kinetics.

In addition to studies of cooperativity and the effects of manipulated duty ratio and n_H the pathway from dissociated to strongly bound actomyosin complexes (figure 15) was studied using phosphate *in vitro* motility assays. Myosin concentration was varied over a control curve and a

phosphate curve with 30mM phosphate (figure 11). This study shows that with low concentrations of myosin both the control and phosphate curve show highly similar velocities. This trend is followed until we reach a myosin concentration of 0.1 mg/ml at which point we begin to see a divergence in the velocity of the phosphate curve as the control curve velocity continues to increase and maintains a higher velocity than the phosphate curve (figure 11). Data points for both the phosphate and control curves were collected at the same concentrations of myosin to ensure accurate comparisons. The highest velocity reached in the control curve is 1.85 while the highest velocity in the phosphate curve is 1.24 at a myosin concentration of 0.05 mg/ml and 0.1 mg/ml respectively.

N,N'p-phenylenedimaleimide (pPDM) is thought to be a structural analogue of myosin S-1 that forces actin-myosin binding to occur in a weakly bound transition state. This means that we increase the number of ionic interactions between actin and myosin essentially creating a drag force that inhibits sliding velocity. This would theoretically shift the pCa_{50} in a rightward direction towards an increase in calcium concentration to achieve half maximal activation of the thin filament. This is shown to be the case in pPDM pCa curves in which the pCa_{50} was equal to 4.91 (figure 12) as opposed to a control without pPDM with pCa_{50} being 6.17 (figure 6).
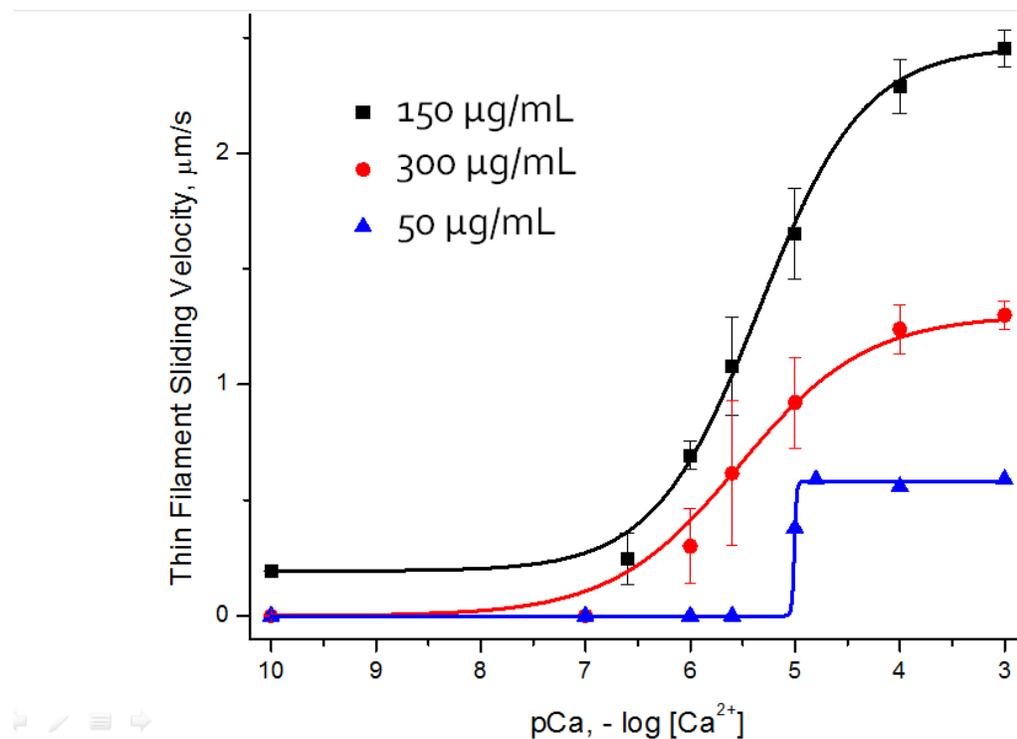
Figure 1. N Dependence of Cooperativity. This figure shows a varying concentration of myosin in µg/ml with changing calcium concentration plotted against an average velocity of the thin filament in an *in vitro* motility assay. The assay was done in triplicate for each concentration of myosin and values were fit using a growth sigmoidal/Rose Dep function.
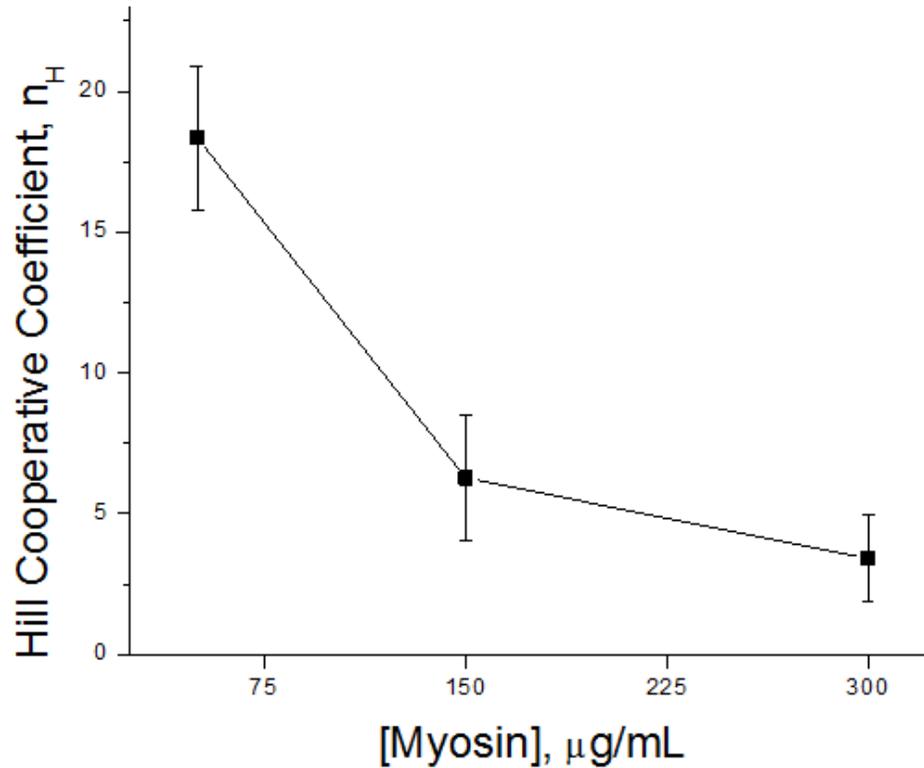
Figure 2. Cooperative Coefficients in Varying Myosin Concentration. This figure shows the calculated Hill coefficients for pCa curves of varying myosin density. Concentration of myosin is measured in µg/ml and plotted against the Hill Coefficient. Curves were done in triplicate and velocities at each pCa value for each concentration of myosin were averaged. Thus slope values are averages of three contributing curves for each plotted concentration of myosin.
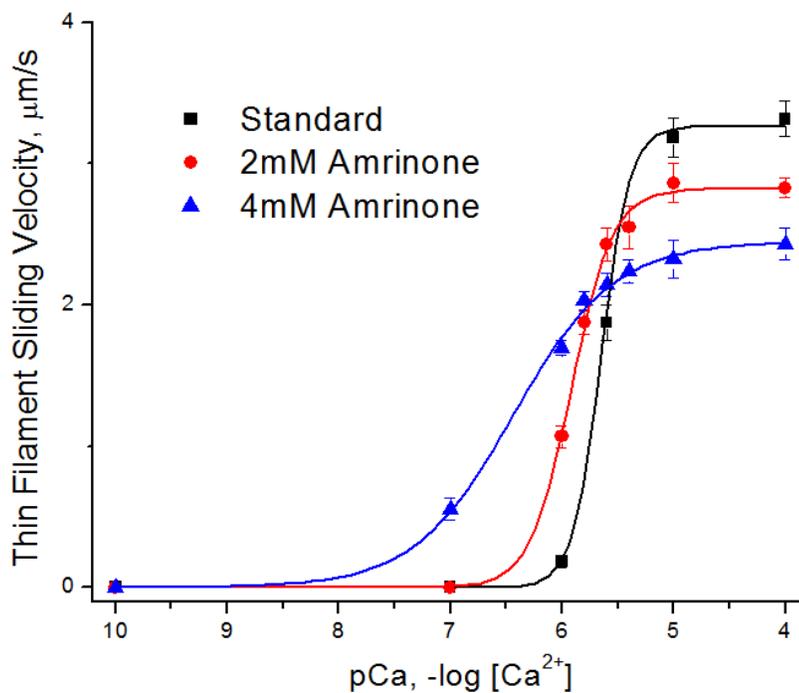
Figure 3. Duty Ratio Dependent Cooperative Activation. Figure 3 shows a control pCa curve and pCa curves with 2mM and 4mM amrinone plotted against the sliding velocity of the thin filament over a bed of myosin heads. Curves were done in triplicate and averaged values were fit using a growth/sigmoidal function. Concentration of calcium is given in a −log scale.
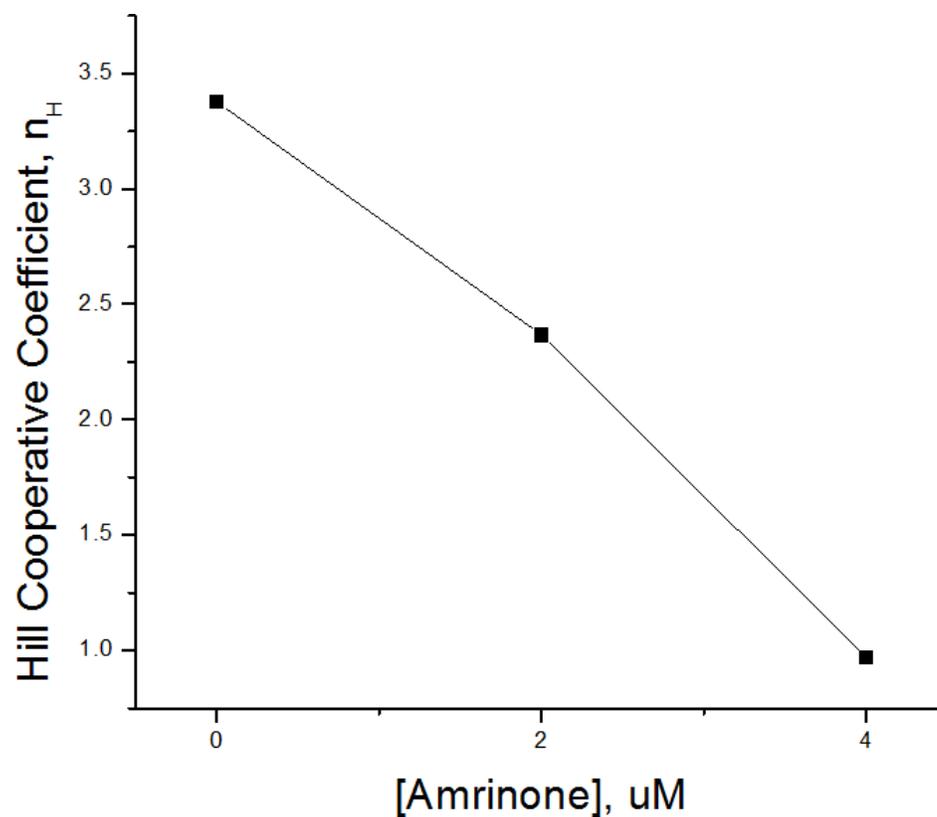
Figure 4. Calculated Hill Coefficients of Amrinone pCa Curves. Hill coefficients were calculated from corresponding slope values in figure 3. These were plotted against concentration of amrinone in µM. Motility assays were done in triplicate thus slope values were averaged across three pCa curves. Hill coefficients are calculated averages of these slopes.
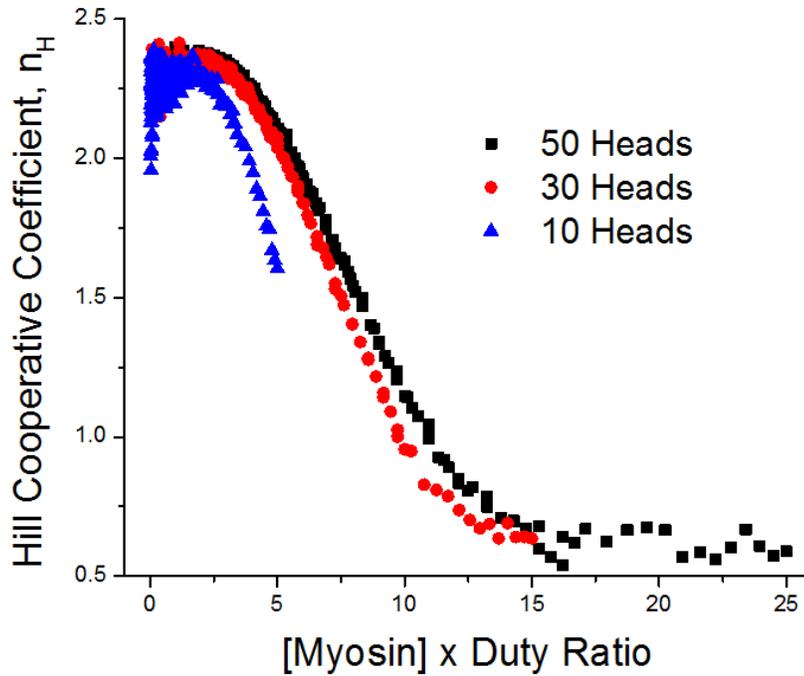
Figure 5. Cooperative Coefficient as Predicted by SCoR. This figure shows the predicted effect of concentration of myosin multiplied by the duty ratio on the Hill cooperative coefficient n_H. This is a predicted compilation of the concepts in figures two and four. Each concentration of myosin, blue being 10 head, red being 30 heads, and black being 50 heads, has the same number of output values and these were calculated using computer simulations of the SCoR model of actomyosin kinetics.
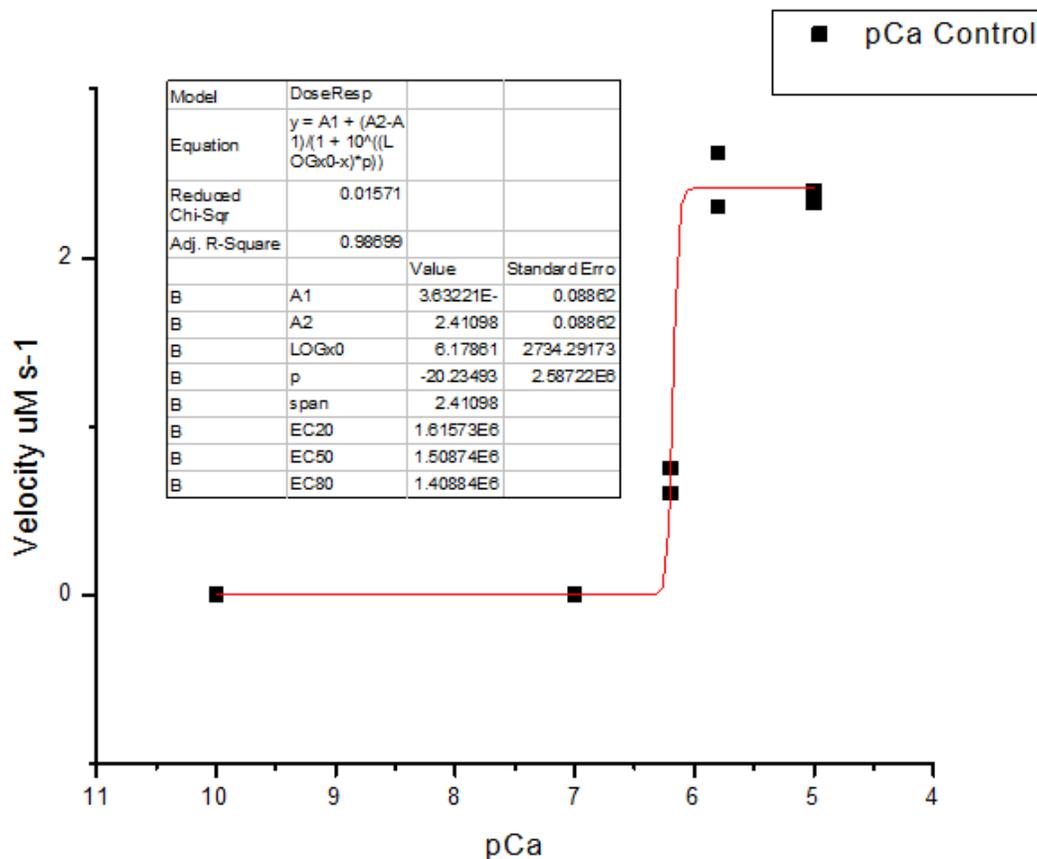
Figure 6. pCa Control Curve. This figure shows the concentration of calcium plotted against the velocity of actin thin filaments. The myosin concentration in this curve is kept at a constant with only the concentration of calcium varied. The corresponding table contains the calculated values of pCa50 and the slope. These are equal to 6.17 and 20.3 respectively. Concentration of calcium varies on a -log scale.
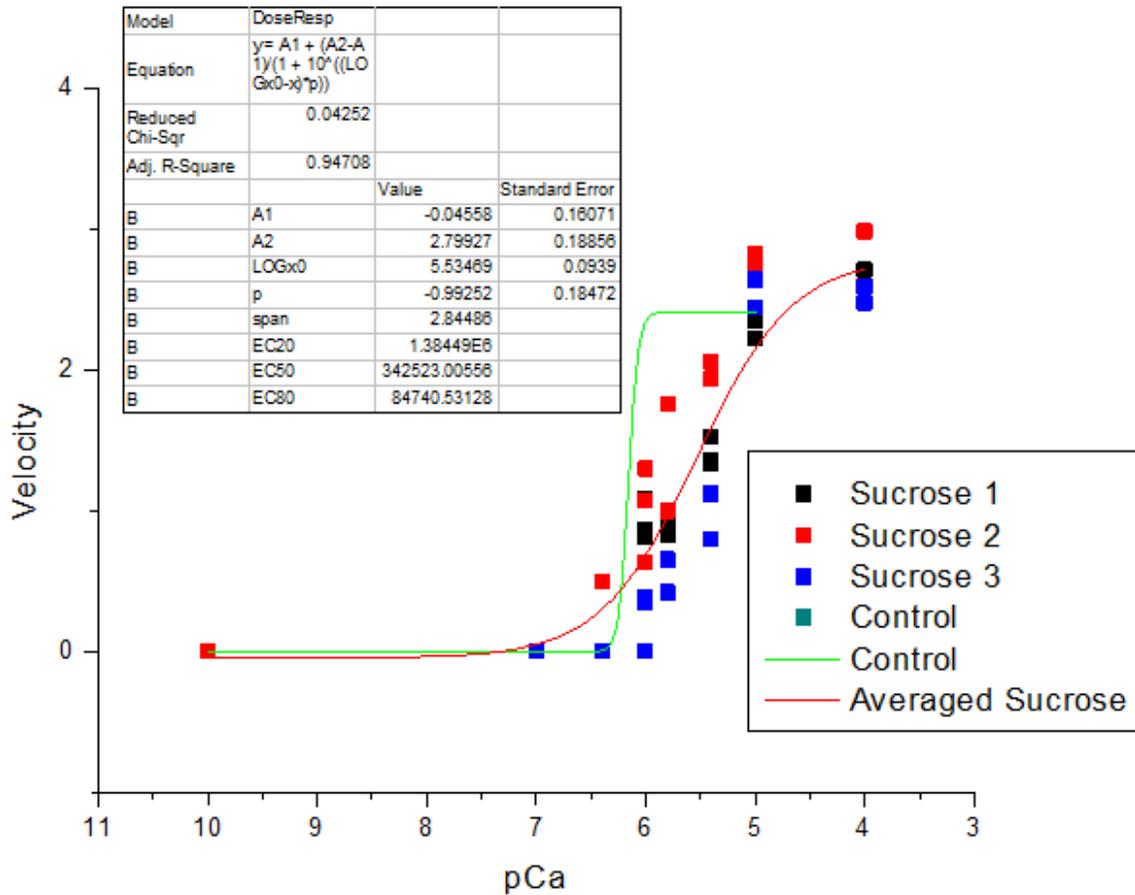
Figure 7. Compiled Sucrose Curves. Figure 7 shows the compilation of three different sucrose pCa curves in which sucrose was added to the motility tube of an in vitro motility assay and the concentration of calcium was varied and plotted against the velocity of the thin filament. The pCa50 value corresponds to LOGx0 in the table and is equal to 5.57 while the slope is 1.13 given by the p value in the table.
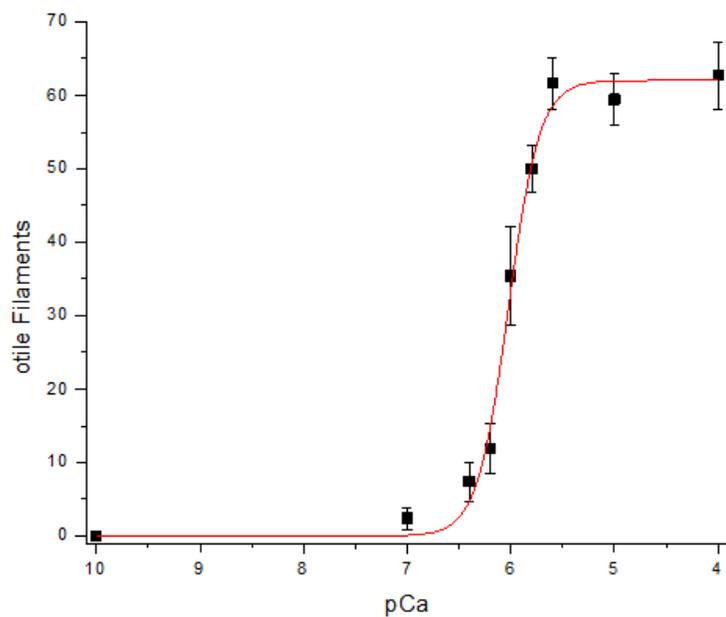
Figure 8. Percent Motile Filaments in Varying Concentration of Calcium. This shows the %
of moving filaments in a pCa control curve. Filaments were counted during a single frame. The
number of moving filaments were counted by advancing and retreating the film by 5-10 frames
on each side of the original frame. Each concentration of calcium required three different
original frames and values were averaged.
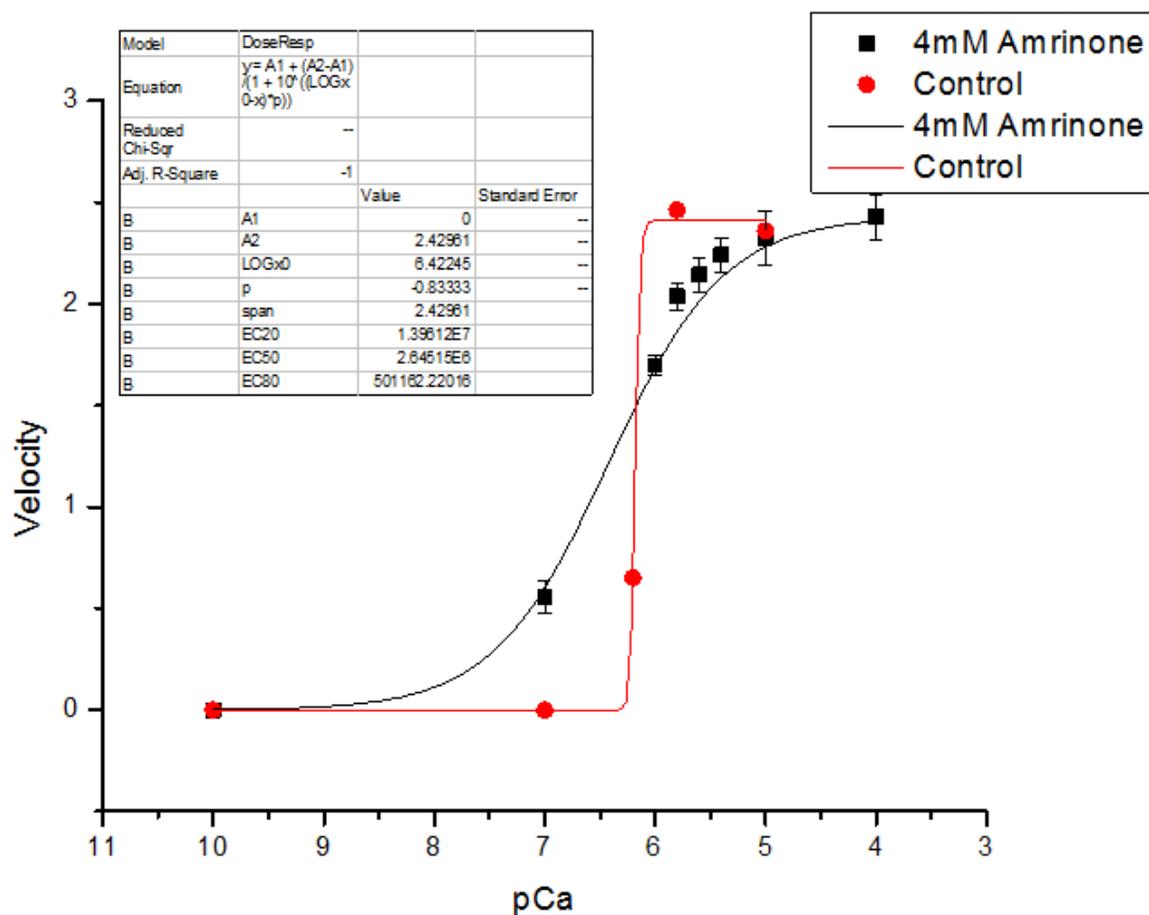
Figure 9. 4mM Amrinone pCa Curve. Figure 9 shows a varying concentration of calcium plotted against velocity. Curves were done in triplicate and averaged into this graph. The motility tube contains 4mM amrinone. pCa_{50} value is 6.42 with a slope value of 1. Data was fit using a Rose/Departure function.
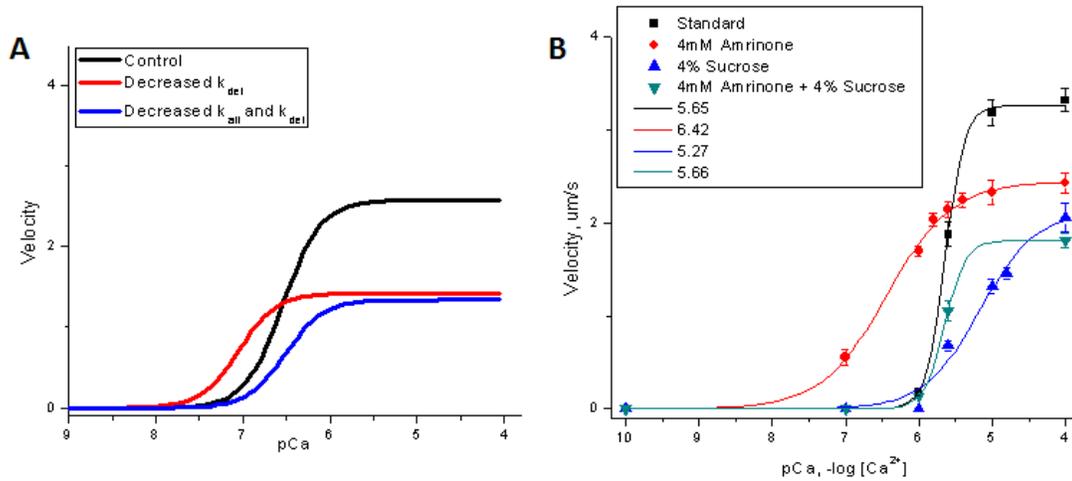
Figure 10. Sucrose Recovery of Calcium Sensitivity. A) Shows the predicted effects of decreased k_{det} and decreased k_{det} and k_{att} as predicted by SCoR and their effects on actin sliding velocities. B) Shows a more complex manipulation of attachment detachment kinetics with use of 4mM amrinone and rescue by sucrose to return pCa50 values to 5.64 and 5.66. This is consistent with SCoR showing that altering both attachment (sucrose) and detachment (amrinone) kinetics can restore calcium sensitivity.
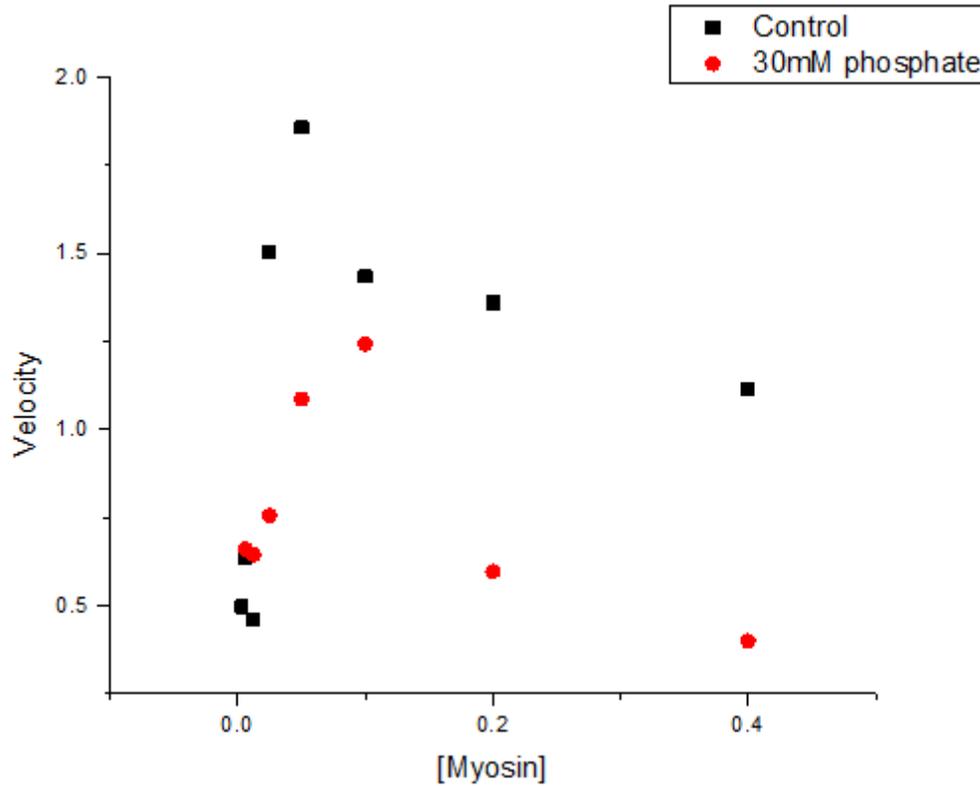
Figure 11. Phosphate Effect on Actin-Myosin Binding Pathway. This figure shows the effect of phosphate (red squares) on thin filament velocities with varying myosin density against a control (black squares). The phosphate curve contains a $30mM$ concentration of phosphate which was added to the motility tube. Both of these curves are unregulated and thus lack TmTn and Calcium. Myosin concentrations are given in mg/ml.
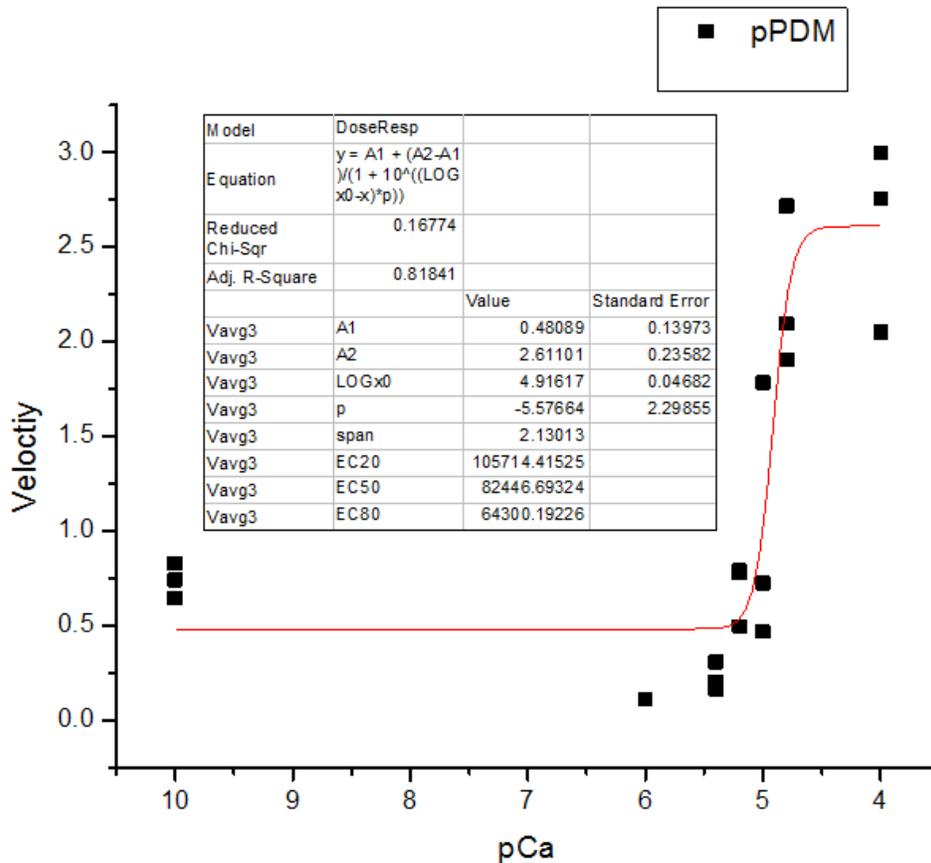
Figure 12. pPDM Effect on pCa50. Shows the effect of *N,N'p*-phenylenedimaleimide (pPDM) in modified myosin S-1 on pCa50 of a pCa *in vitro* motility assay. pCa50 is equal to 4.91 with a slope of 5.57 as calculated by the Rose/Departure fit. Varying calcium concentration is plotted against the velocity of the thin filament. pPDM is thought to be a structural analogue of myosin subfragment-1 that encourages a weakly bound transition state between actomyosin strong binding.
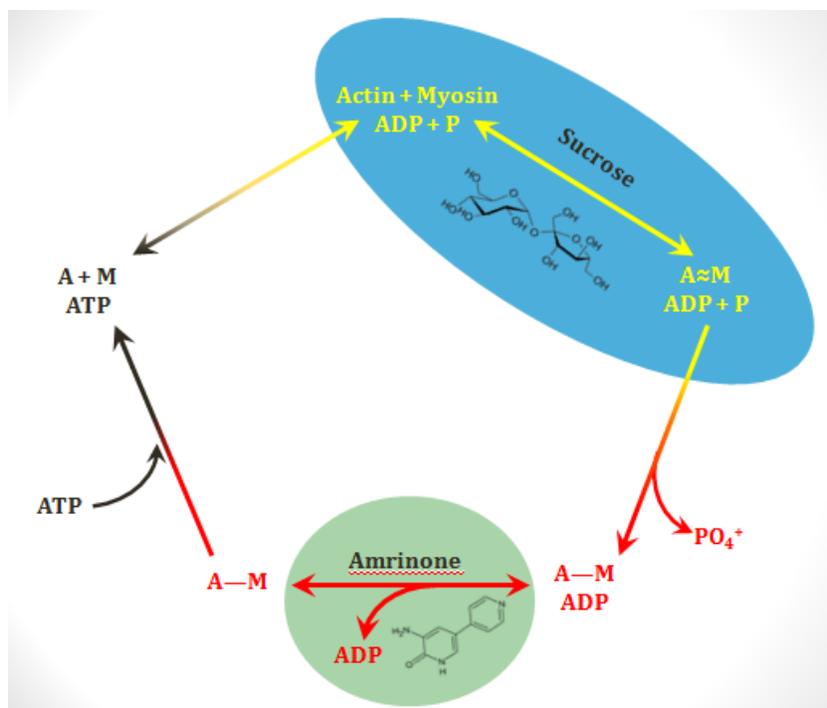
Figure 13. ATPase Cycle of Actomyosin Binding as Affected by Sucrose and Amrinone. Amrinone is known to be an ADP release inhibitor which prolongs the strongly bound state while sucrose is believed to affect attachment kinetics by inhibiting a weak to strong transition. Amrinone and high density myosin are expected to increase the lifetime of a strongly bound state while sucrose and low myosin density are expected to increase the lifetime of a weakly bound state. Yellow denotes a weakly bound state or transition, red denotes a strongly bound state or transition and black denotes a detached state.
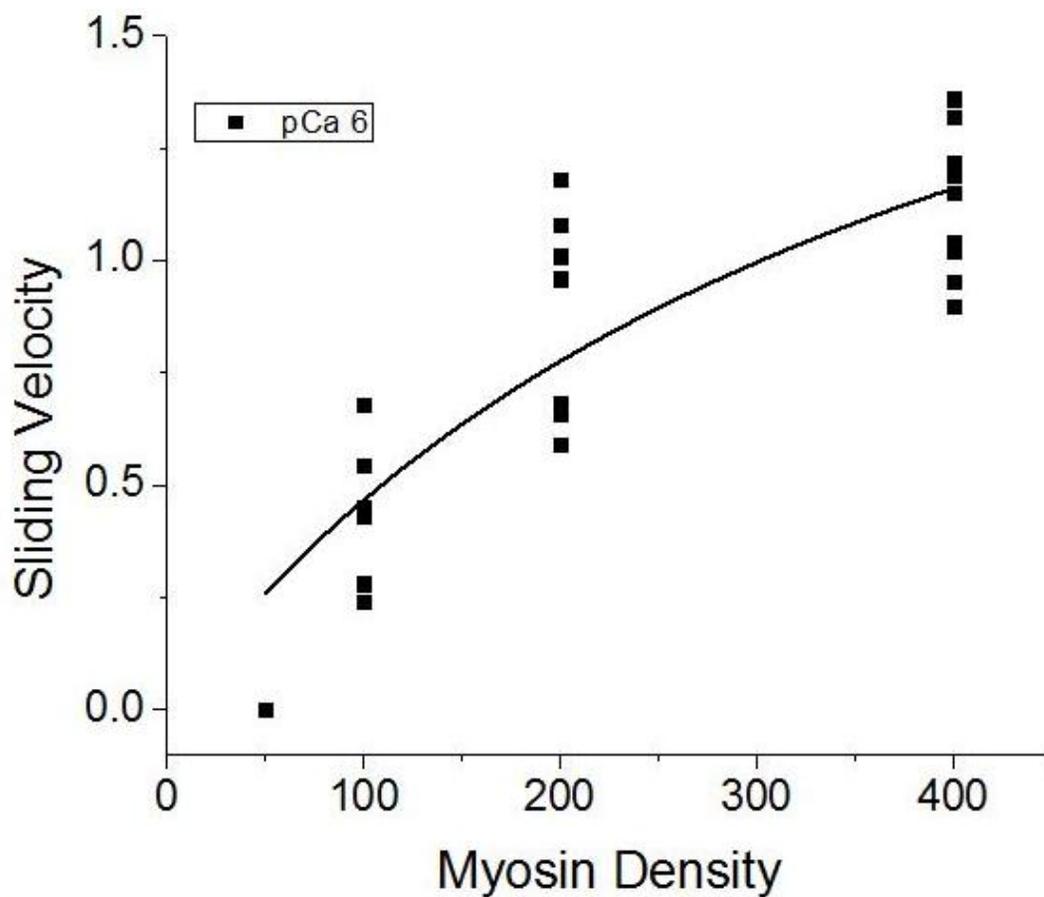
Figure 14. Myosin Density Induced Recovery of Activation at Subactivating Calcium. This figure shows a varying density of myosin at a constant calcium concentration of pCa6. This is plotted against the sliding velocity of an actin thin filament in an *in vitro* motility assay. pCa6 is generally considered to be a subactivating concentration of calcium in *in vitro* motility. Myosin concentrations are given in number of heads available to bind.
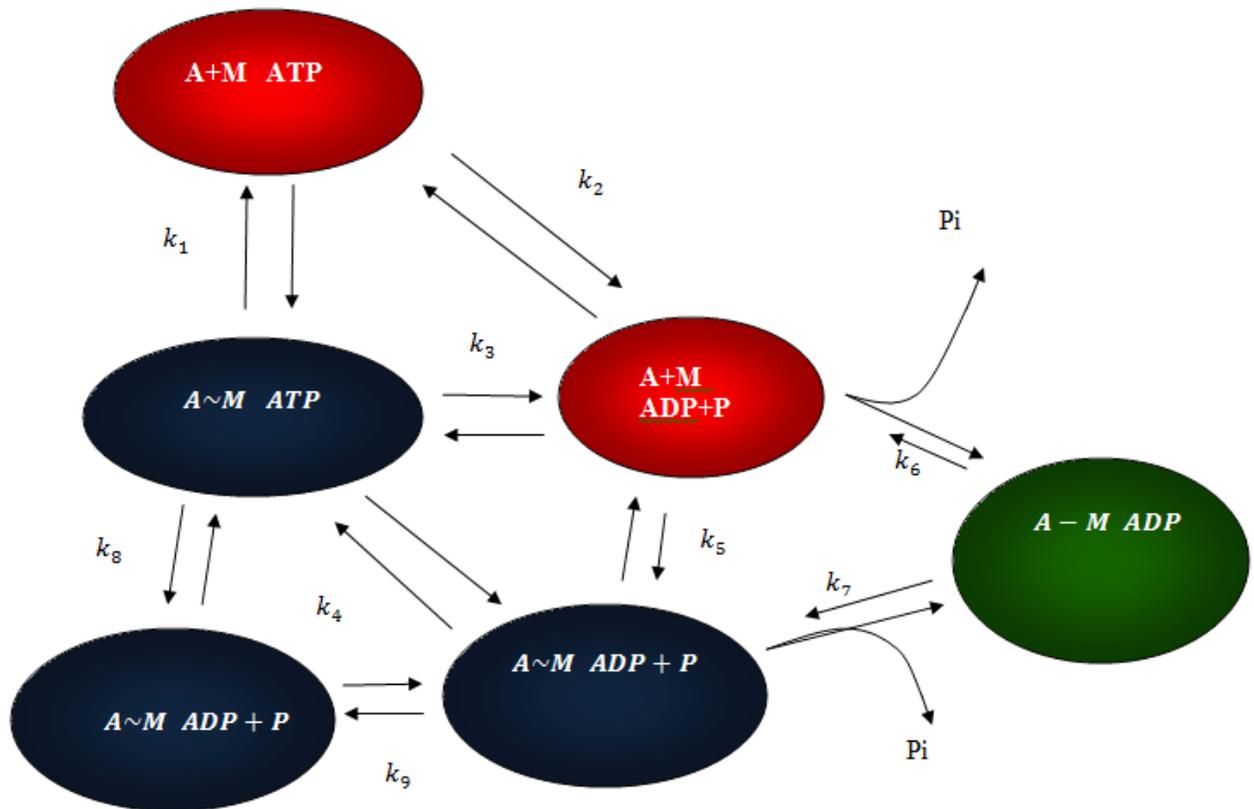
Figure 15. Actin-Myosin Binding Pathways and Equilibriums. This figure shows the various equilibriums that actin and myosin with ATP, ADP, and phosphate form during dissociated, weakly bound, and strongly bound states. The red pathway shows a progression in which actin and myosin transition from dissociated to strongly bound (green circle). The blue pathway denotes a weak binding intermediate state between dissociation and strong binding. Phosphate release allows transition to a strongly bound state.

Discussion-

The effects of actin-myosin ATPase kinetics on the regulation of the thin filament and the

pathway by which this cycle operates are not well understood. The goal of this thesis is to

improve the description of these kinetic properties and the effects they have on cooperativity in

muscle contraction as well as define which parts of this cycle can be affected by various

inhibitors. In addition an insight into the weakly bound transition state is provided through the

use of phosphate *in vitro* motility assays. To this effect we have developed a model (SCoR) in

which these parameters can be changed and predicted accurately to describe a linearly varying

relationship between pCa_{50} and the myosin duty ratio (r). We must first demonstrate the ability

of myosin to activate the thin filament at subactivating calcium concentrations (figure 14). This

shows that at a pCa of six (subactivating) a high myosin density can activate the thin filament

which is seen in the increased sliding velocity as the concentration of myosin is increased. Thus

myosin is capable of activating the thin filament in addition to calcium activation. This allows us

to discuss cooperativity and duty ratio with the goal that changing these parameters can affect

change in muscle contraction. Cooperativity n_H varies with r (figure 5). We then establish a

basis for the effect of k_{att} on pCa_{50} as it can be changed by inhibitors of k_{att} (figure 7) and can

even recover calcium sensitivity lost by the addition of amrinone (figure 10). Taken together

these results suggest that k_{det} and k_{att} can both affect the calcium sensitivity or pCa_{50} of thin

filament activation. The number of myosin heads N, available to bind has also been shown to

affect pCa_{50} (16). This attains physiological relevance in the peak function (figure 5) that is seen

at low $\cdot r$. This figure describes the effect a protein modification or modification that alters duty

ratio and subsequently lowers the cooperative coefficient has on the amount of calcium

transported into the cell to achieve contraction. Namely that such a change would require a

greater amount of calcium to achieve muscle contraction which could in turn place a metabolic

strain on the cell. However, it is important to note that calcium sensitivity cannot be indefinitely

increased by addition of compounds such as sucrose. First of all myosin duty ratio cannot

theoretically exceed one. Secondly at finite values of N curves begin to saturate. In addition there

are only so many myosin binding sites on actin which would also limit the calcium sensitivity of

the system as these sites become saturated or as myosin heads spend longer and longer times in a

strongly bound state.

The SCoR model of activation attempts to describe the related effects of $n_H, k_{att}, k_{det}, pCa_{50}$

and N which no current model does (13). Simulations suggest there is a linear relationship

between pCa_{50} and $N \cdot r$ (13). We use this model to predict a relationship between $N \cdot r$ and the

cooperativity coefficient of myosin binding (figure 5). This suggests that maximum cooperativity

is reached near physiological duty ratios (figure 4). Cooperativity is constrained by n_t (figure 1

and 2). This shows us that cooperative activation is not only calcium dependent but is also

dependent on the concentration of myosin or duty ratio which is $\cong \frac{n_b}{n_t}$ where n_b is the number of

myosin heads bound divided by the total number of myosin heads available n_t. Not only is duty

ratio affected by amrinone but so too is overall velocity, and thus activation of the thin filament

(figure 3). This is likely due to the notion that amrinone is an inhibitor of ADP release and thus

the rate of detachment. This means that each strongly bound myosin head would, in effect,

remain bound longer with increasing concentration of amrinone. An increase in the number of

strongly bound heads would slow the overall ATPase cycle slowing velocity. This increase in the

number of strongly bound heads makes it more likely that at least one head remains bound at any

one time allowing the next binding event to occur in an unregulated or calcium insensitive

fashion. This is why we see a decrease in calcium sensitivity with increase in amrinone

concentration (figure 9). Taken together figures 2, 4, 7, 9, and 10 confirm the hypothesis that

ATPase kinetics tune calcium sensitivity and effect cooperativity of myosin binding (amrinone

affects k_{det}) and (sucrose affects k_{att}).

Cooperativity and calcium sensitivity become physiologically relevant in their ability to increase

and decrease the amount of calcium the cell must move in and out to achieve muscle contraction.

The more calcium one must move in and out to achieve contraction the greater the metabolic

strain such movement places upon the cell. In many cardiomyopathies this can become a

compounding problem in which cells must progressively move in and out greater and greater concentrations of calcium as loss of function occurs elsewhere in the muscular contraction system. To calculate the cooperative coefficients of myosin binding (figures 2 and 4) a cooperative relationship had to be assumed requiring our curve analysis to be a Hill fit. Additionally the relationship between velocity and activation or k_{att} is likely more complicated than what we assume in saying that velocity is a direct measure of activation of the thin filament.

There continues to be a debate over whether or not the weak binding state of actin-myosin is indeed on the pathway to the strongly bound state (15). We explore this in figures 11 and 15. Figure 11 shows the effect of phosphate on the velocity of the thin filament with varying myosin density against a control (which only varies myosin density). The addition of phosphate should push the equilibrium towards the actin, myosin, ADP, phosphate state. If the weakly bound state was able to transition immediately and quickly to the strongly bound state thus activating the thin filament we would expect to see an increase in the overall rate of the ATPase cycle. This would mean a faster velocity as we would be increasing the cycling of the myosin heads binding and unbinding on the actin filaments. As shown in figure 11 this is not quite the case. The control and phosphate curves initially start at the same velocities but quickly diverge with the phosphate velocity decreasing quickly as we raise the concentration of myosin. This seems to suggest that the weak binding state can saturate thus slowing velocity. This suggests that there are multiple weak binding transition states formed and that only from a select few can actin and myosin transition to a strongly bound productive state. Therefore with a load inducing concentration of myosin we see these weakly bound states formed and as they become saturated they alternate between each other at a rate of k_9 and between weakly bound and dissociated at a rate of k_5 or k_1 (figure 15). As shown in figure 15 there could potentially be many equilibriums between

weak and dissociated, and weak and strong binding some of which would be more favorable than others. This would create a decrease in velocity at high myosin concentrations with phosphate addition due to a shift in equilibrium towards a weakly bound blue state (figure 15). An alternative hypothesis would be a transition from a dissociated to strongly bound state without the intermediate weak interactions. This pathway to strong binding is shown in red (figure 15). We further test these weak interactions with the use of pPDM modified myosin S-1. pPDM myosin is known to increase the number of weakly bound myosin heads meaning that to achieve contraction one would need to move more calcium into the cell overcoming the ionic drag created by such weak binding events. As shown in figure 12 we see an increase of pCa_{50} to 4.91. This is significantly more calcium than what is required in the control curve with pCa_{50} of 6.17. The drastic increase in calcium needed for half maximal activation suggests that the weak binding state is not holding tropomyosin off the actin binding sites or increasing the number of heads able to transition to the strongly bound state but rather that if found in a weakly bound state myosin heads are unable to progress to strongly bound easily. This much larger amount of calcium suggests the need for largely calcium dependent activation and not weak to strong transitioning. It should be noted here that more analysis is needed to make greater determinations on the nature of weak binding saturation and transition pathways. For instance although ionic strength can be accounted for with the addition of phosphate by changing concentration of KCl it should be noted that this is a difference in the type of ions that we did not control for. It could be that an addition of phosphate could interact with an amino acid residue inside the binding domain of the S-1 subfragment thereby inhibiting binding in a manner we did not discuss.

Here we have discussed the ability of myosin to bind cooperatively to actin and shown that modulating the duty ratio and number of available heads can shift this cooperativity with changes

in myosin concentration or use of inhibitors like amrinone. In addition we have shown the

effectiveness of the SCoR model of actomyosin binding kinetics and discussed the ways in

which duty ratio and N bound can tune calcium sensitivity. Finally we have proposed an

alternative to the transition between weakly and strongly bound through the use of pPDM and

phosphate. The further study of these effects could lead to advancements in the treatment of

cardiomyopathies, the macroscale modeling of muscle contraction, and loss of function mutation

known to place metabolic strains on cardiac and skeletal muscle.

Bibliography

1. Klinth, J., Arner, A., and Månsson, A. (2003) Cardiotonic bipyridine amrinone slows myosin-induced actin filament sliding at saturating [MgATP], *Journal of muscle research and cell motility*. Springer *24*, 15–32.
2. Potter, J. D. (1982) [22] Preparation of troponin and its subunits, *Methods in enzymology*. Elsevier *85*, 241–263.
3. Smillie, L. (1982) Preparation and Identifaction of Alpha and Beta Tropomyosins, in *Methods in enzymology*, pp 234-241.
4. Prochniewicz, E., Lowe, D., Spakowicz, D. J., Higgins, L., O'Conor, K., Thompson, L. V., Ferrington, D. A., and Thomas, D. D. (2008) Functional, structural, and chemical changes in myosin associated with hydrogen peroxide treatment of skeletal muscle fibers, *American Journal of 294*, C613-26.
5. Margossian, S. S., and Lowey, S. (1982) Preparation of myosin and its subfragments from rabbit skeletal muscle, in *Methods in Enzymology* (Colowick, S. P., and Kaplan, N. O., Eds.), pp 55-71. Academic Press, New York.
6. Pardee, J. D., and Spudich, J. A. (1982) Purification of muscle actin, *Methods in enzymology*. Elsevier *85*, 164–181.
7. Swartz, D. R., Moss, R. L., and Greaser, M. L. (1996) Calcium alone does not fully activate the thin filament for S1 binding to rigor myofibrils., *Biophysical journal 71*, 1891-904.
8. Huxley, H. (1973) Structural Changes in the Actin-and Myosin-containing Filaments during Contraction, *Cold Spring Harbor Symposia on Quantitative Biology 37*, 361-376.
9. Haselgrove, J. (1973) X-ray evidence for a conformational change in the actin-containing filaments of vertebrate striated muscle, *Journal of Molecular Biology* 549-568.
10. Parry, D. (1973) Structural role of tropomyosin in muscle regulation: analysis of the x-ray diffraction patterns from relaxed and contracting muscles, *Journal of molecular biology 75*, 33-55.
11. Squire, J. (1994) The actomyosin interaction-shedding light structural events: "Plus ca change, plus c"est la meme chose', *Journal of muscle research and cell motility 231*, 227-231.
12. Herzberg, O., and James, M. (1985) Structure of the calcium regulatory muscle protein troponin-C at 2.8 angstrom resolution, *Nature 313*, 653-659.
13. Webb, M., Jackson, D., Stewart, T., Dugan, S., Carter, M., Fears, M., Cremo, C., Baker, J . (2012) A simple concerted model of thin filament regulation: How actin-myosin kinetics fine tune calcium sensitivity
14. K. Kirshenbaum, S. Papp, and S. Highsmith (1993) Cross-linking myosin subfragment 1 Cys-697 and Cys-707 modifies ATP and actin binding site interactions. *Biophysical Journal* 1121-1129
15. Brenner, B., Schoenberg, J.M. Chalovich, L.E. Greene, and E. Eisenberg. (1982) Evidence for Cross-bridge attachment in Relaxed Muscle at low Ionic Strength. *Proc. Natl. Acad. Sci.* 7288-7291
16. Gorga, J., Fishbaugher, D., and VanBuren, P. (2003) Activation of the calcium-regulated thin filament by myosin strong binding, *Biophysical Journal.* Elsevier 85, 2484–2491.